

# Geophysical Research Letters<sup>®</sup>

## RESEARCH LETTER

10.1029/2021GL095102

### Key Points:

- The initial emergence of dry patches in nonrotating radiative-convective equilibrium is insensitive to cloud-radiation interaction
- Strong cloud forcing is necessary for sustained dry patch growth and the realization of convective self-aggregation
- Circulation feedback is initially negative and restrains self-aggregation but becomes positive as dry patches grow to substantial sizes

### Supporting Information:

Supporting Information may be found in the online version of this article.

### Correspondence to:

X. Shi,  
[shixm@ust.hk](mailto:shixm@ust.hk)


### Citation:

Fan, Y., Chung, Y. T., & Shi, X. (2021). The essential role of cloud-radiation interaction in nonrotating convective self-aggregation. *Geophysical Research Letters*, 48, e2021GL095102. <https://doi.org/10.1029/2021GL095102>

Received 7 JUL 2021

Accepted 15 SEP 2021

## The Essential Role of Cloud-Radiation Interaction in Nonrotating Convective Self-Aggregation

Yiyuan Fan<sup>1</sup>, Yu To Chung<sup>1</sup>, and Xiaoming Shi<sup>1</sup> 

<sup>1</sup>Division of Environment and Sustainability, Hong Kong University of Science and Technology, Hong Kong, China

**Abstract** Convective self-aggregation in radiative-convective equilibrium (RCE) is a phenomenon of significant interest because of its potential relevance to the organization of tropical storms. However, some previous theories on RCE instability neglected or simplified cloud-radiative interaction in theoretical models and suggested that water vapor-radiation feedback is responsible for destabilizing a homogeneous RCE state. Here, through numerical experiments of nonrotating RCE, we first confirm that the predictions from these theories are valid inasmuch that dry patches can form in an initially homogeneous domain with uniform sea-surface temperature when cloud-radiation interaction is suppressed or eliminated. However, sustained growth of those dry patches is not guaranteed. Developing deep convective circulation can engulf dry patches, and water vapor feedback is not sufficient for overcoming this barrier. Only when the early-stage cloud radiative forcing is sufficiently strong can self-aggregation fully develop. Therefore, cloud-radiative feedback is essential for the eventual realization of self-aggregation in nonrotating RCE.

**Plain Language Summary** Radiative-convective equilibrium (RCE) refers to a balanced atmospheric state with radiative cooling and moist convective heating, a representative idealization of the tropical atmosphere. In RCE simulations, a homogeneous initial state may spontaneously evolve into an inhomogeneous state in which convective clouds cluster in a moist region and are surrounded by dry air. This spontaneous development of organized convection is termed convective self-aggregation and is thought to be relevant to the organization of tropical weather systems. Convective self-aggregation starts with the formation of small dry patches in the simulation domain. Previous theories explained their emergence as the result of water vapor-radiative interaction constrained by atmospheric dynamics. In this study, we find that those theories neglecting cloud-radiative feedback are only partially correct. After the initial formation of dry patches, the developing deep convection in moist regions may engulf those dry patches due to the downgradient transport of moisture and energy. Only when the cloud-radiative feedback is sufficiently strong can the barrier due to deep convective circulation be overcome. Thus, cloud-radiative interaction is essential for the complete development of self-aggregation and is of great practical importance because clouds are infamous for their uncertainties.

## 1. Introduction

Radiative-convective equilibrium (RCE) is defined by the balanced conditions under which radiative cooling in the atmosphere of an idealized domain is compensated by convective heating (e.g., Stephens et al., 2008; Tompkins & Craig, 1998). In their two-dimensional cloud-resolving simulations, Held et al. (1993) first discovered the tendency of convective cells in RCE to aggregate spontaneously into a localized cluster of convective clouds. They suggested that the moisture field facilitates this localization by providing the memory of convection. Bretherton et al. (2005) referred to this phenomenon in RCE as *convective self-aggregation*, which has since been studied extensively in three-dimensional cloud-resolving models (see a review by Wing et al. [2017]).

The development of self-aggregation involves the interaction among multiple physical processes, including radiation, convective circulation, cloud microphysics, boundary layer turbulence, and surface fluxes (Wing et al., 2017). However, to understand the RCE instability, simplified theoretical models have been developed (Beucler & Cronin, 2016; Bretherton et al., 2005; Emanuel et al., 2014). Among the authors of those studies, Emanuel et al. (2014) developed a two-layer atmospheric model that can represent the interaction among moisture, radiation, and circulation. Their analysis suggests that RCE instability occurs through the interaction between circulation and clear-sky radiation when the sea surface temperature (SST) exceeds a

threshold. Others (Beucler & Cronin, 2016; Bretherton et al., 2005) chose to ignore the details of three-dimensional circulation and developed theories based on the governing equation of the vertically integrated frozen moist static energy (iMSE), leading to simpler and more transparent results.

Denoting the iMSE by  $H$ , its governing equation in RCE can be expressed as

$$\frac{\partial H}{\partial t} = R + F + A, \quad (1)$$

where  $R$  is the radiative forcing,  $F$  is the surface enthalpy flux, and  $A$  is the transport due to advection. Bretherton et al. (2005) empirically parameterized these three terms on the right-hand side, with  $R$  and  $F$  depending on the cloudiness and gustiness caused by convection and  $A$  depending on the mode (shallow or deep) of convection. In all three terms, convection is measured by the precipitation anomaly. Nevertheless, although they parameterized the coarsening effect (countergradient transport) (Craig & Mack, 2013) of shallow convection in relatively dry regions, the effect of advection still causes the diffusion of iMSE anomalies on average; therefore, their model predicts that the sensitivity of  $(R + F)$  to convection needs to be large enough to amplify iMSE perturbations.

Beucler and Cronin (2016) further simplified the problem by ignoring the advection term and assuming that the surface flux is constant. Then, by linearizing the resulting equation with respect to a base state, the governing equation becomes

$$\frac{\partial H'}{\partial t} = R' = \frac{\overline{\partial R}}{\partial H} H', \quad (2)$$

where the overline denotes the base RCE state, and the prime denotes a deviation from the base state. They further assumed that  $H'$  is dominated by moisture perturbations; therefore, the equation above is equivalent to

$$L_v \frac{\partial q'}{\partial t} = R' = \frac{\overline{\partial R}}{\partial q} q', \quad (3)$$

where  $q$  denotes the column-integrated water vapor. In Equation 3, the moisture perturbation grows exponentially if the sensitivity of radiation with respect to moisture is positive, i.e.,  $\overline{\partial R / \partial q} > 0$ . The analysis of Beucler and Cronin (2016) suggests that, above a certain threshold of  $q$ , such an instability can indeed occur in the atmosphere, and they termed this mechanism *moisture-radiative cooling instability* (MRCI).

Thus, all these theoretical models assume that radiative feedback plays a critical role in destabilizing the homogeneous nonrotating RCE state. However, while it is recognized that cloud-radiative feedback eventually dominates during the mature stage of self-aggregation (Wing & Emanuel, 2014), the authors mentioned above disagree on whether cloud- or moisture-radiation interaction is more crucial in initially triggering the RCE instability. This study analyzes cloud-resolving simulations employing differing cloud microphysics schemes with varying cloud ice characteristics or amounts. The results demonstrate that cloud-radiative feedback is critical for the occurrence of self-aggregation, not because MRCI cannot initialize the separation of moist and dry anomalies but because early-stage dry patches may be engulfed by moist convection around them as the circulation develops. Intense cloud radiative forcing is necessary for overcoming this barrier to allow the unrestrained development of self-aggregation.

## 2. Model and Methods

### 2.1. Cloud-Resolving Model

Our simulations used Cloud Model 1 (CM1) (Bryan & Fritsch, 2002), Release 20.2. CM1 is a nonhydrostatic cloud-resolving model that includes state-of-the-art physical parameterizations. The setup of initial conditions follows that of Bretherton et al. (2005). The SST is uniform and fixed at 301 K. The incoming top-of-atmosphere (TOA) solar radiation is held constant at  $650.83 \text{ W m}^{-2}$ . Radiative transfer is computed with the Rapid Radiative Transfer Model for general circulation models (RRTMG) (Iacono et al., 2008). Boundary-layer turbulence is modeled with a Louis-type scheme (Bryan & Rotunno, 2009). The horizontal grid spacing is 3 km, and the vertical grid spacing ranges from 50 m near the surface to 500 m in the upper levels. The horizontal and vertical spans of the simulation domain are 648 km and 28 km, respectively. All

simulations are integrated over 40 days, which is shorter than the 100-day (or more) integration in other studies but sufficient for our discussion to focus on the early stages of convective self-aggregation.

## 2.2. Cloud Microphysics

We first conducted simulations with two different cloud microphysics schemes, the Morrison scheme (Morrison et al., 2009) and the Thompson scheme (Thompson et al., 2008). The former is a two-moment bulk microphysical model that predicts both the masses and the number concentrations of cloud and precipitation species; the latter includes double-moment ice and rain and an improved representation of snow processes. The CM1 simulation using the Morrison scheme initially exhibits the formation of dry patches in the domain, but these dry patches subsequently disappear. In contrast, the Thompson scheme simulation exhibits dry patches sustained until the end of the simulation.

We next focused on the Morrison scheme to test the impacts of varying cloud ice amounts and thereby varying cloud-radiative feedback. One convenient parameter in the Morrison scheme to tune the cloud ice concentration is the threshold size for cloud ice autoconversion; this parameter is named DCS in the code. It has been demonstrated that cloud radiative forcing is quite sensitive to the value of DCS (Eidhammer et al., 2014; Zhao et al., 2013), and smaller values of DCS can lead to the more efficient removal of cloud ice. The default DCS value is 125  $\mu\text{m}$ . In addition to this default value, we multiply it by factors of 0.2, 0.5, 2, and 5 to obtain four additional experiments that, in later discussion, are referred to as DCS 0.2, DCS 0.5, DCS 2.0, and DCS 5.0, respectively.

## 2.3. Frozen Moist Static Energy

Our analysis mainly focuses on the iMSE. Frozen moist static energy is a conserved variable in moist adiabatic processes and is defined as

$$h_f = c_p T + gZ + L_v q_v - L_f q_i, \quad (4)$$

where  $c_p$  is the specific heat at constant pressure,  $T$  is temperature,  $g$  is the gravitational constant,  $Z$  is the geopotential height,  $L_v$  and  $L_f$  are the latent heats of vaporization and sublimation, respectively, and  $q_v$  and  $q_i$  are the specific ratios of water vapor and cloud ice, respectively. The iMSE ( $H$ ) is the vertical integral of  $h_f$  from the bottom to the top of the atmospheric column,

$$H = \int \rho h_f dz. \quad (5)$$

The budget equation for the iMSE is given by Equation 1. It should be noted that  $R$  in this equation denotes the net heating of a column due to radiation; therefore, negative values of  $R$  represent radiative cooling of the column.

In some analyses, we used block averaging to focus on mesoscale processes, following Bretherton et al. (2005). Mesoscale blocks are the results of horizontally partitioning the domain into  $9 \times 9$  ( $72 \times 72 \text{ km}^2$  each) blocks and horizontally averaging the data within each block.

## 3. Results

### 3.1. Two Microphysics Schemes

Figure 1 shows the distributions of the water vapor path (WVP) in the simulations using the default Morrison and Thompson microphysics schemes on Days 20 and 40. The early development is similar in both simulations. On Day 20, both simulations exhibit the formation of small dry patches with WVP of 10–15 mm in the domain, surrounded by moist regions with WVP of approximately 35 mm. However, on Day 40, all dry patches disappeared in the Morrison simulation, with a quasi-homogeneous distribution of the WVP at  $\sim 30$  mm. In contrast, in the Thompson simulation, the smaller dry patches merge into a single large dry patch, which is sustained throughout the simulation.

Therefore, the contrast between these two simulations suggests that the early-stage formation of dry patches is not highly sensitive to the subtle differences between the two microphysics schemes. In and around

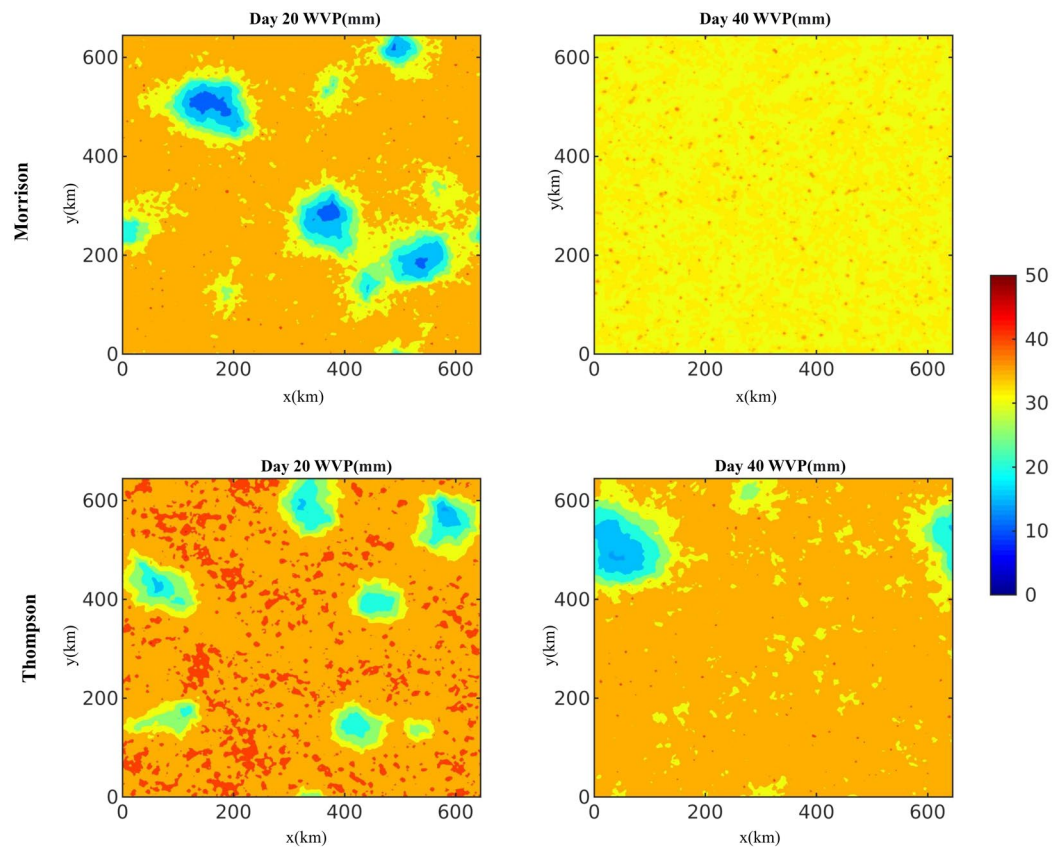


**Figure 1.** Snapshots of the water vapor path (WVP) fields in the simulations using the Morrison (upper row) and Thompson (lower row) microphysics schemes. The left column displays the WVP fields on Day 20, and the right column displays those on Day 40. The Morrison run used the default DCS value.

these dry patches, shallow circulation forms and supports the development of self-aggregation by triggering the upgradient transport of the iMSE (Bretherton et al., 2005; Muller & Held, 2012; Muller & Bony, 2015). On Day 20, the dry regions exhibit stronger radiative cooling than the moist regions, and this contrast alone promotes the amplification of iMSE anomalies. However, the initial formation of dry patches does not guarantee the further growth of these anomalies. An examination of the surface enthalpy fluxes on Day 20 suggests no significant difference between these fluxes in dry and moist regions. Therefore, the circulation (A) is mainly responsible for the later disappearance of dry patches in the Morrison simulation.

Furthermore, an examination of the TOA cloud radiative forcing suggests that the cloud radiative effect is quite different between the two simulations (Figure S1). In particular, the TOA longwave cloud forcing in the Thompson simulation appears to be significantly stronger than that in the Morrison simulation in moist regions. The vertical distribution of cloud ice has some notable differences between these two simulations, albeit not substantial. The dramatically different effective size of cloud ice between the two microphysics schemes appears to be the dominant factor for their difference in cloud forcing (Figure S2): the effective size of cloud ice in the Morrison scheme is  $\sim 3$  times larger than that in the Thompson scheme, making the optical depth of clouds smaller in the former. Thus, it is most likely that the stronger cloud radiative forcing helps amplify the iMSE anomalies in the Thompson simulation and allows the dry patches to survive the adverse effect of advection.

### 3.2. Adjusting Cloud Ice

This section analyzes the simulations using the Morrison scheme but with varying DCS values. Smaller DCS values lead to the more efficient conversion of cloud ice into frozen precipitation (snow and graupel). This approach allows us to tune the cloud radiative forcing in the experiments without directly changing the

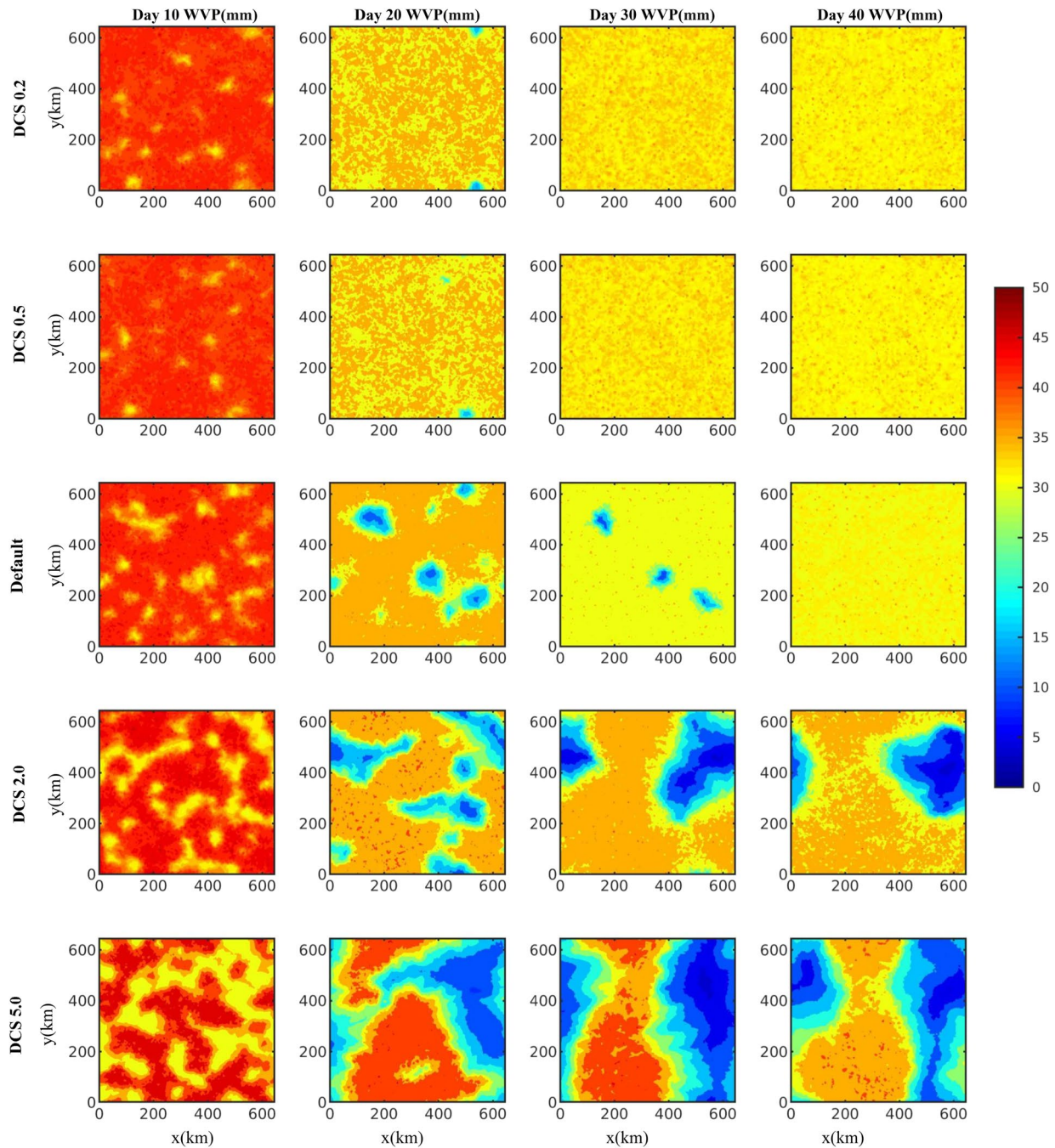


**Figure 2.** Snapshots of the water vapor path fields in the simulations using the Morrison microphysics scheme but with different DCS values (smaller DCS values in the upper rows). The columns are for Days 10, 20, 30, and 40 from left to right.

latent heating inside convective cores or changing the particle size distribution assumptions in the Morrison scheme.

Figure 2 shows the distributions of the WVP in these simulations at different times. On Day 40, the DCS 2.0 and DCS 5.0 simulations exhibit partially completed self-aggregation, whereas the other simulations on Day 40 exhibit quasi-homogeneous WVP distribution. However, on Days 10 and 20, dry patches have formed in the domain in all simulations despite having different sizes and intensities. In the case of DCS 5.0, the dry patches occupy a larger area than in the other simulations, and on Day 20, the intensities of the dry and moist regions contrast at 10 and 45 mm, respectively, and the dry patches occupy approximately half of the

**Table 1**  
*Estimation of the Radiative and Circulation Feedback Strengths by Linear Regression*

Experiment	Feedback	Day 10	Day 20	Day 30	Day 40
DCS 0.2	$R_H$	0.78	0.564	0.76	0.78
DCS 0.2	$A_H$	- 6.89	- 12.85	- 55.42	- 57.59
DCS 0.5	$R_H$	0.98	0.69	0.92	0.76
DCS 0.5	$A_H$	- 9.99	- 18.28	- 53.29	- 58.09
Default	$R_H$	1.07	0.62	0.82	1.17
Default	$A_H$	- 2.41	- 0.91	- 3.00	- 53.28
DCS 2.0	$R_H$	1.23	0.65	0.59	0.57
DCS 2.0	$A_H$	- 0.68	0.21	0.46	0.23
DCS 5.0	$R_H$	1.26	0.69	0.64	0.60
DCS 5.0	$A_H$	- 0.58	- 0.06	1.17	0.82

*Note.*  $R_H$  Denotes  $\overline{\partial R/\partial H}$  and is Estimated by regressing the net radiative forcing anomalies ( $R'$ ) onto the iMSE anomalies ( $H'$ ) in mesoscale blocks.  $A_H$  Denotes  $\overline{\partial A/\partial H}$  and is estimated by regressing the advection tendency anomalies ( $A'$ ) onto the iMSE anomalies ( $H'$ ) in mesoscale blocks. Data from 24-h periods are used for computing the regression coefficient for each day. The unit for both  $R_H$  and  $A_H$  is  $10^{-6}\text{s}^{-1}$ .  $A$  is computed implicitly as the residual of the budget equation for each 3-h period.

domain. In the DCS 0.2 simulation, the dry patches on Day 20 are small in size, but the intensities of the dry patches and moist regions are 15 and 35 mm, respectively, the difference between which is still relatively large. The other simulations exhibit in-between behaviors.

Therefore, we again show that dry patches can be initiated regardless of the cloud microphysics scheme details (referring to cloud ice here), but the growth rate and later survival of those dry patches are sensitive to variations in the details of clouds. Changing DCS values does not significantly alter cloud fraction at low levels (below ~3 km) but introduces a substantial change in middle and high levels (Figure S3). For example, on Day 10, mid-level and high cloud fraction in DCS 5.0 is approximately 0.2–0.3, whereas, in DCS 0.2, it is smaller than 0.03. Due to the differing cloud coverage, these simulations do not have the same RCE energy balance, in that their radiative cooling and latent heating are different. By Day 40, the differences in domain-averaged precipitation in these simulations are approximately 10% (Figure S4).

#### 4. Feedbacks

Our analysis above suggests that completely ignoring the advection term in Equation 1 can lead to a significant underestimation of the RCE instability threshold. Even though the initial condition of most RCE simulations is a horizontally uniform domain, for which advection does not contribute much to the tendency of the iMSE, the circulation strength is enhanced as dry patches form and grow. If we choose to retain the advection term in the iMSE budget equation and linearize it, we obtain

$$\frac{\partial H'}{\partial t} = R' + A' = \frac{\overline{\partial R}}{\partial H} H' + \frac{\overline{\partial A}}{\partial H} H'. \quad (6)$$

The surface enthalpy flux term is ignored because we did not intentionally manipulate the relevant calculation, and in general, the surface flux feedback plays a lesser role in nonrotating convective self-aggregation (Wing et al., 2017).

Linearizing these two terms might oversimplify actual physical processes because the circulation strength cannot be uniquely determined by the iMSE only, and the same can be said about radiation when clouds are considered. However, Equation 6 allows us to semiquantitatively understand and compare the effects of radiative and circulation feedbacks. Using mesoscale block averages of the anomalies of  $H$ ,  $R$ , and  $A$ , we can estimate the feedback strengths  $\overline{\partial R/\partial H}$  and  $\overline{\partial A/\partial H}$  through linear regression. The results are shown in Table 1.

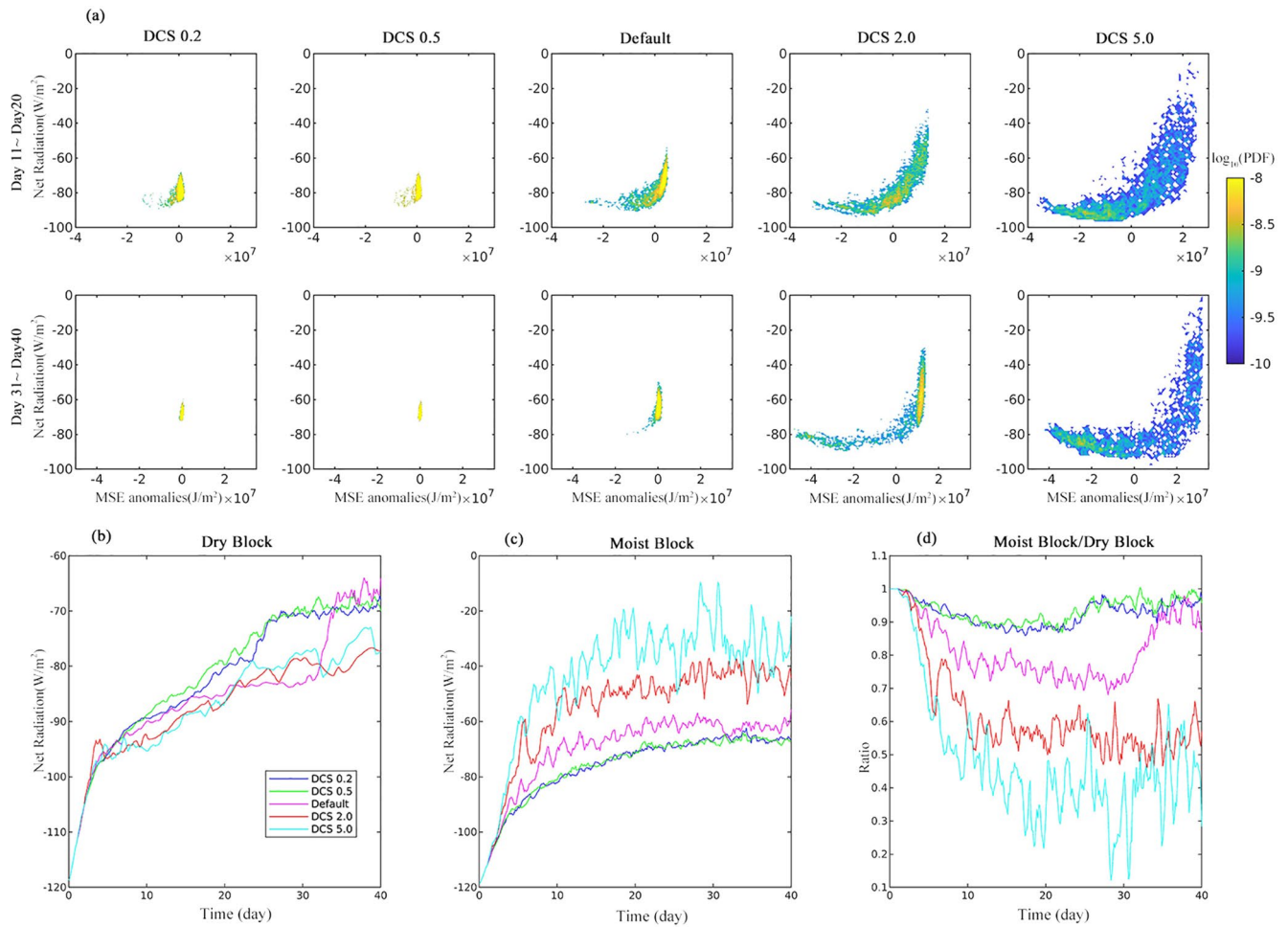


**Figure 3.** Net radiative heating in the simulations. The panels in (a) show the logarithm of the probability distribution function for net radiative heating and integrated frozen moist static energy anomalies of mesoscale blocks between Days 11–20 (upper row) and Days 31–40 (lower row); different columns correspond to the simulations with different DCS values. (b) and (c) are the net radiative heating time series in the driest and moistest blocks, respectively, (d) is the time series for the ratio of the net radiative heating in the moistest blocks to that in the driest blocks. The time series in (b)–(d) are smoothed with a three-point (9-h) running average.

In the five simulations with varying DCS values, the radiative feedback  $R_H$  is always positive. At the early stage (Day 10), the simulations with more cloud ice (DCS 2.0 and DCS 5.0) exhibit stronger radiative feedback. However, near the end, those simulations with sustained self-aggregation exhibit weaker radiative feedback than they did earlier. This transition is due to the ineffectiveness of enhancing radiative cooling in dry regions (see the discussion below about Figure 3). A similar weakening of  $R_H$  is observed in the other three simulations (DCS 0.2, DCS 0.5, and Default) on Day 20.

The circulation feedback strength ( $A_H$ ) exhibits a large range of variability throughout the simulations. At the early stages,  $A_H$  is negative for all simulations, but the difference between the simulations is already substantial ( $A_H$  is stronger in the DCS 0.2 and DCS 0.5 simulations than in the others). At the later stages,  $A_H$  becomes positive in the DCS 2.0 and DCS 5.0 simulations; thus, the circulation promotes self-aggregation, which is due to the shallow circulation around the dry regions, thereby causing upgradient transport of iMSE. In contrast, in the other three simulations,  $A_H$  becomes strongly negative ( $\sim -50$ ) and makes the development of self-aggregation impossible, given that  $R_H$  is only  $\sim 1$ . This strong negative circulation feedback in the simulations without sustained self-aggregation is probably due to the growth of convectively coupled waves, which reside on a fast manifold of unstable modes in RCE (Kuang, 2018). Figure S5 shows the eddy kinetic energy of vertical motions, which becomes a few times larger at the end of the DCS 0.2 and DCS 0.5 simulations than that in the DCS 2.0 and DCS 5.0 runs. Given that the atmosphere in the simulations

without sustained self-aggregation is convectively energetic and that the iMSE anomalies are weak, it is not surprising that the circulation feedback in those simulations becomes strongly negative.

The full complexity of the radiative feedback is revealed in Figure 3. Figure 3a shows the dependence of the net radiative heating (negative values indicate cooling) on the iMSE anomalies as joint probability distribution functions (PDFs) of the two. The DCS 0.2 and DCS 0.5 simulations exhibit a smaller range of variability in terms of both radiation and the iMSE, especially between Days 31 and 40 when the domain becomes quasi-homogeneous. However, between Days 11 and 20, weak iMSE anomalies exist in these two simulations and correspond to relatively strong radiative cooling. The Default simulation exhibits similar characteristics, with larger variability at early stages than later stages. The DCS 2.0 and DCS 5.0 simulations exhibit significantly larger variability due to the robustness of their dry patches. Interestingly, in the dry regions (weak iMSE anomalies), the intensity of radiative cooling is relatively homogeneous, suggesting that the variation in the radiative cooling due to changes in water vapor only is relatively small. Near the left end of the PDFs, the distribution displays a downward slope. This reversed slope is consistent with the analysis of Beucler and Cronin (2016). They showed that under dry conditions, radiative cooling weakens as column water vapor decreases; because as the amount of moisture in the atmosphere decreases, the TOA outgoing longwave radiation continues to increase, but the downward longwave flux from the atmosphere to the surface also decreases due to reduced emissivity of the atmosphere.

Clouds are mainly responsible for the contrast between the net radiation in dry and moist regions. As shown in Figure 3a, at the early stage in the DCS 5.0, DCS 2.0, and Default simulations, radiative cooling can be significantly weakened in moist regions (right end of the PDFs). The net radiation in moist regions shows a long vertical span for a relatively narrow range of iMSE anomalies, reflecting the uncertainty in cloud distribution for given iMSE. The upper end of the PDFs can be as weak as  $\sim 20 \text{ W m}^{-2}$ , whereas the lower bound of the net radiative cooling in moist regions can be as strong as  $\sim 80 \text{ W m}^{-2}$ , which is only slightly weaker than the strongest radiative cooling in the domain.

The strength of radiative cooling in the moistest and driest blocks and their ratios are shown in Figures 3b–3d. The radiative cooling in the moistest blocks weakens over time due to the increased cloud cover during the simulations. However, in later stages, the variation in the radiative cooling of the moistest blocks stabilizes, even in the simulations without successful self-aggregation. In contrast, the radiative cooling in the driest blocks continues to weaken throughout the simulations. This trend is due to the reduced emissivity in the drying atmosphere.

The ratio of radiative cooling in the moistest blocks to that in the driest is a good measure of the strength of differential radiative forcing, with smaller ratios indicating stronger differential heating across the domain. In the DCS 2.0 and DCS 5.0 simulations, the ratios drop quickly with time and stabilize at  $\sim 0.5$ . The DCS 0.2 and 0.5 simulations exhibit ratios as low as 0.9 around Day 25 but show increases to unity between Days 25 and 30, during which the dry patches disappear. The Default simulation also shows initial decreases, but a later increase to unity occurs relatively quickly between Days 30 and 35.

The variability in the ratio of moist-to-dry block radiative cooling is dominated mainly by moist-block clouds. In the driest blocks (Figure 3b), the difference in net radiation between different simulations is always smaller than  $15 \text{ W m}^{-2}$ , and before Day 20, the difference is approximately  $5 \text{ W m}^{-2}$  or smaller. In contrast, the difference in the moistest blocks between different simulations (Figure 3c) reaches  $50 \text{ W m}^{-2}$  on Day 20. The ice cloud water path (IWP), liquid cloud water path (LWP), and WVP are compared in Figure S6, in which we find that at least for the early stage (approximately before Day 20), the WVP and LWP are very similar among the simulations, while the IWP exhibits dramatic contrasts.

## 5. Summary and Discussion

Some previous linear theories on nonrotating RCE instability ignored cloud-radiation interaction and suggested that moisture-radiative feedback is the dominant factor in destabilizing the homogeneous nonrotating RCE state. Our simulations using different cloud microphysics schemes support the conclusions from those theoretical models inasmuch that all of our simulations exhibit the formation of dry patches in the homogeneous domain at the early stage, although the areas and intensities of these dry patches differ.



However, not all simulations can sustain the growth of dry patches. The diffusing effect of circulation forms a second barrier that can potentially terminate the development of convective self-aggregation. Before the dry patches become substantial in size, the circulation triggers the downgradient transport of iMSE and tends to suppress the growth of dry patches. In dry regions, radiative cooling does not strengthen substantially as the WVP decreases, and the dependence of radiative cooling on the WVP is weak and may even be reversed (a drier atmosphere is characterized by weaker cooling). Thus, the development of dry patches can potentially weaken the strength of radiative feedback and eventually allow the negative feedback of circulation to dominate. Then the atmosphere becomes convectively energetic, making the resurgence of self-aggregation impossible.

The cloud-radiation interaction is thus essential for determining whether the development of convective self-aggregation can overcome the second barrier in nonrotating RCE. When a microphysics scheme produces stronger cloud radiative forcing, it substantially weakens the radiative cooling in moist regions and produces stronger differential radiative heating across the domain. If the resulting radiative feedback is strong enough to overcome the barrier due to dynamics, the negative advection feedback ( $A_H$ ) can be weakened or even become positive, removing the barrier to the further development of self-aggregation.

Although our experiments alter the ice-phase cloud radiative forcing, the results shall not be interpreted as suggesting that low clouds are unimportant. Indeed, previous studies have suggested that low cloud-induced longwave cooling at the cloud top drives the shallow circulation around dry patches (Muller & Held, 2012; Muller & Bony, 2015). Because of the inadequate resolution of convection-permitting simulations, the low-cloud process causes additional dependence on model resolution, domain size, and turbulence parameterization (Muller & Held, 2012; Tompkins & Semie, 2017).

Thus, it is unclear whether the dry patches in the DCS 0.2 and 0.5 simulations result from water-vapor or low-cloud radiation interaction. To resolve this ambiguity, we conducted a supplementary simulation in which only clear-sky radiative heating (ignoring clouds) is applied to the temperature field. The results (Figure S7) show that dry patches still form and exist in this “clear-sky” simulation until Day 10, and then gradually disappear. Therefore, at least for the setup of our CM1 simulations, water-vapor radiative feedback is responsible for the initiation of dry patches, while low clouds enhance later dry-patch expansion. The relative importance of low versus high clouds is not our central focus, but we speculate the answer to this question depends on the characteristics of particular cloud microphysics schemes and other model components such as turbulence.

Estimating the linear nonrotating RCE instability threshold based on clear-sky radiation and a homogeneous base state results in a threshold that is likely both too high and too low. The threshold is excessively high in that cloud-radiation interaction can significantly enhance the relative heating in moist atmospheric columns and thereby potentially lower the threshold for the strength of moisture-radiative feedback and is excessively low in that the circulation-induced second barrier is seemingly too difficult to overcome for moisture-radiative feedback alone. Without sufficient cloud forcing, initially developed dry patches can later be engulfed by moist convection surrounding them. The first issue can be addressed by adding a simple parameterization of the cloud effect into theoretical linear models. The second issue is complicated for linear models because the base state needs to include early-stage dry patches and moist region convection, and there is more than one choice for this base state. Although some other details of cloud-circulation interaction are not discussed here (e.g., Bretherton et al., 2005; Muller & Held, 2012; Tompkins & Semie, 2017), we assert that the cloud-radiation interaction is of essential importance for nonrotating RCE instability in practice, especially for its well-known uncertainties in numerical models (e.g., McCoy et al., 2015; Schneider et al., 2017).

### Data Availability Statement

The name list files to reproduce the numerical experiments can be found at <https://doi.org/10.5281/zenodo.5081271>.

**Acknowledgments**

The authors thank Dr. Benjamin Fildier and another anonymous reviewer for their helpful comments and the support by the Research Grants Council of Hong Kong SAR, China (Project Nos. AoE/E-603/18 and HKUST 26305720). The CM1 code was kindly provided by Dr. George Bryan (<https://www2.mmm.ucar.edu/people/bryan/cm1/>).

**References**

Beucler, T., & Cronin, T. W. (2016). Moisture-radiative cooling instability. *Journal of Advances in Modeling Earth Systems*, 8(4), 1620–1640. <https://doi.org/10.1002/2016ms000763>

Bretherton, C. S., Bloussy, P. N., & Khairoutdinov, M. (2005). An energy-balance analysis of deep convective self-aggregation above uniform sst. *Journal of the Atmospheric Sciences*, 62(12), 4273–4292. <https://doi.org/10.1175/jas3614.1>

Bryan, G. H., & Fritsch, J. M. (2002). A benchmark simulation for moist nonhydrostatic numerical models. *Monthly Weather Review*, 130(12), 2917–2928. [https://doi.org/10.1175/1520-0493\(2002\)130<2917:absfmn>2.0.co;2](https://doi.org/10.1175/1520-0493(2002)130<2917:absfmn>2.0.co;2)

Bryan, G. H., & Rotunno, R. (2009). The maximum intensity of tropical cyclones in axisymmetric numerical model simulations. *Monthly Weather Review*, 137(6), 1770–1789. <https://doi.org/10.1175/2008mwr2709.1>

Craig, G. C., & Mack, J. M. (2013). A coarsening model for self-organization of tropical convection. *Journal of Geophysical Research: Atmospheres*, 118(16), 8761–8769. <https://doi.org/10.1002/jgrd.50674>

Eidhammer, T., Morrison, H., Bansemmer, A., Gettelman, A., & Heymsfield, A. J. (2014). Comparison of ice cloud properties simulated by the community atmosphere model (cam5) with in-situ observations. *Atmospheric Chemistry and Physics*, 14(18), 10103–10118. <https://doi.org/10.5194/acp-14-10103-2014>

Emanuel, K., Wing, A. A., & Vincent, E. M. (2014). Radiative-convective instability. *Journal of Advances in Modeling Earth Systems*, 6(1), 75–90. <https://doi.org/10.1002/2013MS000270>

Held, I. M., Hemler, R. S., & Ramaswamy, V. (1993). Radiative-convective equilibrium with explicit two-dimensional moist convection. *Journal of the Atmospheric Sciences*, 50(23), 3909–3927. [https://doi.org/10.1175/1520-0469\(1993\)050<3909:rcewet>2.0.co;2](https://doi.org/10.1175/1520-0469(1993)050<3909:rcewet>2.0.co;2)

Iacono, M. J., Delamere, J. S., Mlawer, E. J., Shephard, M. W., Clough, S. A., & Collins, W. D. (2008). Radiative forcing by long-lived greenhouse gases: Calculations with the aer radiative transfer models. *Journal of Geophysical Research: Atmospheres*, 113(D13). <https://doi.org/10.1029/2008jd009944>

Kuang, Z. (2018). Linear stability of moist convecting atmospheres. part i: From linear response functions to a simple model and applications to convectively coupled waves. *Journal of the Atmospheric Sciences*, 75(9), 2889–2907. <https://doi.org/10.1175/jas-d-18-0092.1>

McCoy, D. T., Hartmann, D. L., Zelinka, M. D., Ceppi, P., & Grosvenor, D. P. (2015). Mixed-phase cloud physics and southern ocean cloud feedback in climate models. *Journal of Geophysical Research: Atmospheres*, 120(18), 9539–9554. <https://doi.org/10.1002/2015jd023603>

Morrison, H., Thompson, G., & Tatarskii, V. (2009). Impact of cloud microphysics on the development of trailing stratiform precipitation in a simulated squall line: Comparison of one-and two-moment schemes. *Monthly Weather Review*, 137(3), 991–1007. <https://doi.org/10.1175/2008mwr2556.1>

Muller, C., & Bony, S. (2015). What favors convective aggregation and why? *Geophysical Research Letters*, 42(13), 5626–5634. <https://doi.org/10.1002/2015gl064260>

Muller, C., & Held, I. (2012). Detailed investigation of the self-aggregation of convection in cloud-resolving simulations. *Journal of the Atmospheric Sciences*, 69(8), 2551–2565. <https://doi.org/10.1175/jas-d-11-0257.1>

Schneider, T., Teixeira, J., Bretherton, C. S., Brient, F., Pressel, K. G., Schär, C., & Siebesma, A. P. (2017). Climate goals and computing the future of clouds. *Nature Climate Change*, 7(1), 3–5. <https://doi.org/10.1038/nclimate3190>

Stephens, G. L., Van Den Heever, S., & Pakula, L. (2008). Radiative-convective feedbacks in idealized states of radiative-convective equilibrium. *Journal of the Atmospheric Sciences*, 65(12), 3899–3916. <https://doi.org/10.1175/2008jas2524.1>

Thompson, G., Field, P. R., Rasmussen, R. M., & Hall, W. D. (2008). Explicit forecasts of winter precipitation using an improved bulk microphysics scheme. part ii: Implementation of a new snow parameterization. *Monthly Weather Review*, 136(12), 5095–5115. <https://doi.org/10.1175/2008mwr2387.1>

Tompkins, A. M., & Craig, G. C. (1998). Radiative-convective equilibrium in a three-dimensional cloud-ensemble model. *Quarterly Journal of the Royal Meteorological Society*, 124(550), 2073–2097. <https://doi.org/10.1256/smsqj.55012>

Tompkins, A. M., & Semie, A. G. (2017). Organization of tropical convection in low vertical wind shears: Role of updraft entrainment. *Journal of Advances in Modeling Earth Systems*, 9(2), 1046–1068. <https://doi.org/10.1002/2016MS000802>

Wing, A. A., Emanuel, K., Holloway, C. E., & Muller, C. (2017). Convective self-aggregation in numerical simulations: A review. *Surveys in Geophysics*, 38, 1173–1197. [https://doi.org/10.1007/978-3-319-77273-8\\_1](https://doi.org/10.1007/978-3-319-77273-8_1)

Wing, A. A., & Emanuel, K. A. (2014). Physical mechanisms controlling self-aggregation of convection in idealized numerical modeling simulations. *Journal of Advances in Modeling Earth Systems*, 6(1), 59–74. <https://doi.org/10.1002/2013ms000269>

Zhao, C., Liu, X., Qian, Y., Yoon, J., Hou, Z., Lin, G., et al. (2013). A sensitivity study of radiative fluxes at the top of atmosphere to cloud-microphysics and aerosol parameters in the community atmosphere model cam5. *Atmospheric Chemistry and Physics*, 13(21), 10969–10987. <https://doi.org/10.5194/acp-13-10969-2013>